
ELSEVIER
APPLIED
OCEAN
RESEARCH

Applied Ocean Research 37 (2012) 111–119

Contents lists available at SciVerse ScienceDirect

Applied Ocean Research

journal homepage: www.elsevier.com/locate/apor

# 3D liquefaction criteria for seabed considering the cohesion and friction of soil

Jianhong Ye[a,b,*]

[a] Key Laboratory of Engineering Geomechanics, Institute of Geology and Geophysics, Chinese Academy of Sciences, Beijing 100029, China
[b] Division of Civil Engineering, University of Dundee, Dundee DD1 4HN, UK

ARTICLE INFO

*Article history:*
Received 28 September 2011
Received in revised form 15 April 2012
Accepted 20 April 2012

*Keywords:*
Liquefaction criteria
Wave loading
Earthquake loading
Cohesion
Friction angle
Porous seabed
Biot's theory

ABSTRACT

In this study, according to the Mohr–Coulomb friction principle, two 3D liquefaction criteria are proposed based on the effective stresses state and the dynamic pore pressure, in which the cohesion and internal friction angle of soil (sand or silt) are both considered. Through the comparison investigation about the liquefaction in soil under wave–current loading, it is found that the cohesion and internal friction angle of soil have significant effect on the prediction of liquefaction zone under dynamic loading, such as wave and earthquake. The new liquefaction criteria proposed in this study can be degenerated to the form proposed by Okusa [16], Tsai [20] and Zen and Yamazaki [26]. It cannot be degenerated to the form proposed by Jeng [9]. It is indicated that there is no clear physical basis for the liquefaction criteria proposed by Jeng [9]. The area and maximum liquefaction depth of liquefaction zone in seabed would be overestimated greatly by the criteria proposed by Jeng [9].



## 1. Introduction

In practice engineering, the liquefaction of soil, especially the non-cohesive sandy soil, under dynamic loading, such as the ocean wave and earthquake, is a widely observed phenomenon. Due to the fact that the liquefied soil behaves like a kind of liquid, there is no any bearing capacity to support the structures built on it. The liquefaction of soil foundation under wave loading and/or earthquake loading potentially is a very dangerous factor for the stability of structures, such as oil platforms, turbines and breakwaters. Some liquefaction induced failure cases of marine structures under wave loading have been reported in previous literature [4,5,14,18,25,27]. The failure of structures due to the earthquake induced liquefaction can be found in Ref. [19]. Therefore, the evaluation of potential liquefaction of soil under dynamic loading is apparently necessary in structures design.

In coastal engineering, there are two types of liquefaction mechanism for the seabed liquefaction: transient liquefaction and residual liquefaction. The transient liquefaction of seabed foundation is mainly related to the phase lag between the dynamic pore pressure in seabed and the dynamic pressure induced by the wave propagating on seabed. The transient liquefaction zones in seabed would appear and disappear periodically in the zone under wave trough. The residual liquefaction is mainly due to the build-up of pore pressure in soil under wave or earthquake loading. Accompanying with the build-up of pore pressure in soil, the contact effective stresses decrease between soil particles. When the contact effective stresses become zero, the soil becomes liquefied. The liquefaction criteria is to state the initial trigger condition of liquefied status of soil, which is very important in evaluation of the liquefaction potential of soil foundation under dynamic loading.

At present, some literatures are available in which some methods are proposed to assess the liquefaction susceptibility of soil under earthquake loading by adopting the parameters of soil property, such as clay content, liquid limit, plasticity index, water content, confining stress [1,2,15,17,21]. However, these methods are all based on engineering experiences; and the high liquefaction susceptibility of soil predicted by these proposed methods does not mean that the soil must be liquefied under earthquake loading. The liquefaction is only a possibility. The experience-based methods for liquefaction susceptibility cannot be used in computation. The quantitative liquefaction criteria is needed in computation to judge whether the soil is liquefied or not. Several works on the quantitative liquefaction criteria are available so far.

Okusa [16] firstly proposed a 1D liquefaction criteria based on the vertical effective stress:

$$-(\gamma_s - \gamma_w)z = \sigma'_{z0} \le \sigma'_{zd} \tag{1}$$

in which the $\gamma_s$ and $\gamma_w$ are the unit weight of soil and water. $z$ is the depth of soil. $\sigma'_{z0}$ is the initial vertical effective stress in seabed. $\sigma'_{zd}$ is the dynamic vertical effective stress induced by the dynamic

* Correspondence address: Division of Civil Engineering, University of Dundee, Dundee DD1 4HN, UK.
*E-mail address:* yejianhongcas@gmail.com

0141-1187/$ – see front matter © 2012 Elsevier Ltd. All rights reserved.
http://dx.doi.org/10.1016/j.apor.2012.04.004

loading. This liquefaction criteria means that if the upward dynamic vertical effective stress is greater than the initial downward effective stress, the soil will liquefy. This criteria has clear physical basis. But the effect of horizontal effective stresses $\sigma'_x$ and $\sigma'_y$ are not taken into consideration. Under the same frame Tsai [20] extended the above 1D liquefaction criteria to 3D condition by adopting the average of the effective stresses:

$$-(\gamma_s - \gamma_w)\left(\frac{1+2K_0}{3}\right) z \le \frac{1}{3}(\sigma'_{xd} + \sigma'_{yd} + \sigma'_{zd}) \tag{2}$$

$K_0$ is the lateral compression coefficient of soil. This liquefaction criteria only adopts the average idea. There is no clear physical meaning of how the horizontal effective stresses $\sigma'_x$ and $\sigma'_y$ affect the liquefaction potential of soil.

Zen and Yamazaki [26] developed another liquefaction criteria based on the dynamic pore pressure:

$$-(\gamma_s - \gamma_w)z = \sigma'_{z0} \le p - p_b \tag{3}$$

in which $p$ and $p_b$ are the dynamic pore pressure in seabed, and the pressure acting on seabed. This liquefaction criteria means that the seabed will liquefy if the upward seepage force can overcome the weight of overburdened soil and/or structures. Similar with the liquefaction criteria proposed by Okusa [16], the physical meaning of this criteria is clear. However, the horizontal effective stresses $\sigma'_x$ and $\sigma'_y$ are also not taken into consideration. Jeng [9] further extended the above liquefaction criteria into 3D situation:

$$-(\gamma_s - \gamma_w)\left(\frac{1+2K_0}{3}\right) z \le p - p_b \tag{4}$$

Similarly, the average idea is used. The physical meaning of how the initial horizontal effective stresses $\sigma'_{x0}$ and $\sigma'_{y0}$ affect the liquefaction potential of soil is not clear.

The above-mentioned four liquefaction criteria all do not take the cohesion and internal friction angle of soil into consideration. From the view of physical phenomenon, the clay with cohesion is more difficult to liquefy than the sand without cohesion; and the dense sand with large internal friction angle is more difficult to liquefy than that of loose sand. Therefore, the effect of cohesion and friction angle on the liquefaction potential of soil is significant and cannot be neglected.

In this study, according to the principle of Mohr–Coulomb friction, two liquefaction criteria based on the effective stresses and pore pressure are proposed, in which the cohesion and internal friction angle of soil (sand or silt) are both considered. The comparison study about the liquefaction in soil under wave–current loading is conducted to illustrate the effect of cohesion and internal friction angle on the liquefied zone in seabed foundation. Some suggestions are also included to demonstrate which liquefaction criteria should be used for various engineering conditions. For the sake of simplicity, the liquefaction criteria proposed by Okusa [16], Zen and Yamazaki [26], Tsai [20] and Jeng [9] are labeled as *A*, *B*, *C* and *D* respectively. The liquefaction criteria proposed in this study considering the cohesion and internal friction angle based on the effective stresses and pore pressure are labeled as *E* and *F*, respectively in the following section.

## 2. Formulation of new 3D liquefaction criteria

### 2.1. Criteria based on effective stresses

It is assumed that there is a micro soil volume ($dx \times dy \times dz$) shown in Fig. 1. At a moment, the effective stress $\sigma'_x$, $\sigma'_y$, $\sigma'_z$, $\tau_{xz}$, $\tau_{yz}$ and $\tau_{xy}$ are acting on the outer surface of the micro soil volume. In this study, the compressive stress is defined as the positive value in analysis, which is widely adopted in soil/rock mechanics.

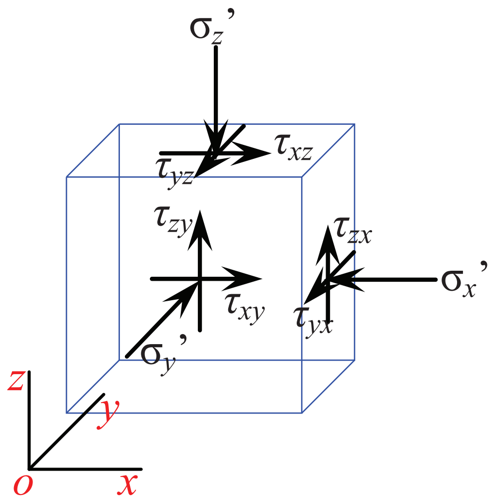


**Fig. 1.** The effective stress state of a micro volume in three dimensions space.

According to the Mohr–Coulomb criteria, the horizontal effective stress $\sigma'_x$, $\sigma'_y$ will provide the friction potential on the four vertical lateral sides to prevent the soil volume from moving upward if the $\sigma'_x$, $\sigma'_y$ are compressive. The friction potential provided by the compressive $\sigma'_x$, $\sigma'_y$ on the lateral sides can be expressed as

$$\begin{cases} 2(c + \sigma'_x \tan\phi)u(\sigma'_x)dydz & \text{induced by} \quad \sigma'_x \\ 2(c + \sigma'_y \tan\phi)u(\sigma'_y)dxdz & \text{induced by} \quad \sigma'_y \end{cases} \tag{5}$$

where the $c$ and $\phi$ are the cohesion and internal fraction angle. $u(x)$ is the unit step function

$$u(x) = \begin{cases} 1 & x > 0 \\ 0 & x \le 0 \end{cases} \tag{6}$$

The usage of the unit step function $u(x)$ in Eq. (5) is to describe that there is no friction potential if the horizontal effective stress $\sigma'_x$, $\sigma'_y$ is tensile ($\le$0).

The vertical effective stress $\sigma'_z$ has two components: the initial vertical effective stress $\sigma'_{z0}$ when there is no dynamic loading, and the dynamic loading induced vertical effective stress $\sigma'_{zd}$. The dynamic loading can be ocean wave or earthquake. The vertical effective stress $\sigma'_z$ should be the sum of initial vertical effective stress $\sigma'_{z0}$ and the dynamic vertical effective stress $\sigma'_{zd}$

$$\sigma'_z = \sigma'_{z0} + \sigma'_{zd} \tag{7}$$

Generally, the initial vertical effective stress $\sigma'_{z0}$ in soil is induced by the self-gravity of soil or/and the gravity of structures built on the soil. Therefore, $\sigma'_{z0}$ is absolutely the resistance for the soil liquefaction. The only probable driven force to make the soil move upward to liquefy is the dynamic vertical effective stress $\sigma'_{zd}$. At one moment, the dynamic vertical effective stress $\sigma'_{zd}$ in soil is compressive, for example, the soil under wave crest, $\sigma'_{zd}$ prevents the liquefaction of soil. However, at another moment, the dynamic vertical effective stress $\sigma'_{zd}$ could be tensile, for example, the soil under wave trough, $\sigma'_{zd}$ will make the soil has the potential to move upward to liquefy. When the tensile $\sigma'_{zd}$ is huge enough to overcome the resistance provided by $\sigma'_x$, $\sigma'_y$ and $\sigma'_{z0}$, the soil will liquefy. Therefore, the liquefaction criteria proposed can be expressed as

$$\begin{aligned} -\sigma'_{zd}dxdy \ge{}& \sigma'_{z0} + 2(c + \sigma'_x \tan\phi)u(\sigma'_x)dydz \\ &+ 2(c + \sigma'_y \tan\phi)u(\sigma'_y)dxdz \end{aligned} \tag{8}$$

or

$$\sigma'_{z0} + \sigma'_{zd} + 2(c + \sigma'_x \tan\phi)u(\sigma'_x)\frac{dz}{dx} + 2(c + \sigma'_y \tan\phi)u(\sigma'_y)\frac{dz}{dy} \le 0 \tag{9}$$

Substituting Eq. (7) into Eq. (9), and considering the $dx = dy = dz$ for the micro soil volume; the liquefaction criteria can be rewritten as:

$$\sigma'_z + 2(c + \sigma'_x \tan\phi)u(\sigma'_x) + 2(c + \sigma'_y \tan\phi)u(\sigma'_y) \le 0 \tag{10}$$

The above proposed 3D liquefaction criteria includes the effect of cohesion and internal friction angle of soil on the liquefaction. It can be degenerated to the criteria proposed by Okusa [16] and Tsai [20]. If the effect of horizontal effective stress $\sigma'_x$, $\sigma'_y$ on the liquefaction is not considered, and the cohesion is set as $c = 0$ for sandy soil, Eq. (10) can be degenerated to 1D stress criteria proposed by Okusa [16]. If the cohesion is $c = 0$, and the friction angle is $\phi = 26.6^\circ$, Eq. (10) can be degenerated to 3D stress criteria proposed by Tsai [20]. It is indicated that the liquefaction criteria proposed by Tsai [20] assume the cohesion $c$ is 0, and the friction of angle $\phi$ of soil is $26.6^\circ$. Clearly, this assumption is inappropriate due to the fact that the friction angle $\phi$ of sandy soil generally is 30–45°; and the cohesion $c$ of clay soil is not 0. The clay soil with significant cohesion is more difficult to liquefy than that of sandy soil. From this view, the effect of cohesion on the liquefaction cannot be ignored.

Comparing the liquefaction criteria based on the effective stresses proposed by Okusa [16] (criteria *A*), Tsai [20] (criteria *C*) and Eq. (10) (criteria *E*) developed in this study, it generally can be inferred that the maximum liquefaction depth predicted by the above three liquefaction criteria has following relationship: $d_A \ge d_C \ge d_E$. $d_A \ge d_C$ is due to the fact that the lateral frictional resistance provided by $\sigma'_x$, $\sigma'_y$ is not included in the liquefaction criteria proposed by Okusa [16]; meanwhile, the lateral frictional resistance is partially considered assuming the friction angle $\phi = 26.6^\circ$ in the liquefaction criteria proposed by Tsai [20]. $d_C \ge d_E$ attributes to that the friction angle of soil is generally is 30–45°, greater than the assumption of $\phi = 26.6^\circ$.

### 2.2. Criteria based on dynamic pore pressure

As illustrated in Fig. 2, a macro 3D soil volume ($\Delta x \times \Delta y \times z$) is chosen as the research object. The wave/earthquake induced dynamic pressure at the top and bottom of soil volume is $p_b$ and $p$. Similar with the liquefaction criteria based on the stresses proposed in above section, the friction potential provided by the initial effective stress $\sigma'_{x0}$, $\sigma'_{y0}$ to prevent the soil volume moving upward can be expressed as

$$\begin{cases} 2(c + \sigma'_{x0} \tan\phi)u(\sigma'_{x0})dydz & \text{induced by} \quad \sigma'_{x0} \\ 2(c + \sigma'_{y0} \tan\phi)u(\sigma'_{y0})dzdx & \text{induced by} \quad \sigma'_{y0} \end{cases} \tag{11}$$

Before the dynamic force is applied to the soil volume, the initial vertical effective stress $\sigma'_{z0}$ induced by the self-gravity of soil and/or gravity of structures built on seabed is also the resistance for the soil liquefaction. The resistance can be expressed as $\sigma'_{z0}dxdy$

After the dynamic force is applied to the soil volume, the vertical seepage force $j_z$ in the soil volume is the only probable driven force making the soil volume move upward to liquefy. when the vertical seepage force is upward, and huge enough to overcome the initial resistance, the soil volume will move upward, and liquefy (the surface of seabed is set as $z = 0$):

$$\begin{aligned} \int_z^0 \int_x^{x+\Delta x} \int_y^{y+\Delta y} j_z dxdydz &\ge \int_x^{x+\Delta x} \int_y^{y+\Delta y} \sigma'_{z0} dxdy \\ &+ \int_z^0 \int_y^{y+\Delta y} 2(c + \sigma'_{x0} \tan\phi)u(\sigma'_{x0})dydz \\ &+ \int_z^0 \int_x^{x+\Delta x} 2(c + \sigma'_{y0} \tan\phi)u(\sigma'_{y0})dzdx \end{aligned} \tag{12}$$

where the seepage force $j_z$ are defined as the gradient of dynamic pressure at the position of the soil volume:

$$j_z = -\frac{\partial p_s}{\partial z} \tag{13}$$

in which $p_s$ is the dynamic pore pressure. The minus sign '−' means that the upward seepage force is taken as positive value.

If the $\Delta x$ and $\Delta y$ is sufficiently small, the $j_z$, $\sigma'_{z0}$, $\sigma'_{x0}$ and $\sigma'_{y0}$ could be considered to be uniform on area $\Delta x \times \Delta y$. Performing the integration for Eq. (12), obtaining

$$\begin{aligned} (p - p_b)\Delta x \Delta y &\ge \sigma'_{z0}\Delta x \Delta y + \Delta y \int_z^0 2(c + \sigma'_{x0} \tan\phi)u(\sigma'_{x0})dz \\ &+ \Delta x \int_z^0 2(c + \sigma'_{y0} \tan\phi)u(\sigma'_{y0})dz \end{aligned} \tag{14}$$

where the $p_b$ and $p$ are the dynamic pore pressure on seabed and in seabed at the depth $-z$. For the seabed without marine structures built on it. The horizontal effective stress $\sigma'_{x0}$ and $\sigma'_{y0}$ in the consolidation status could be approximately expressed as

$$\sigma'_{x0} = \sigma'_{y0} = K_0\sigma'_{z0} = K_0(\gamma_s - \gamma_w)z \tag{15}$$

in which the $K_0$ is the lateral pressure coefficient of soil. Substituting the expression of $\sigma'_{x0}$, $\sigma'_{y0}$ and $\sigma'_{z0}$ in Eq. (15) into Eq. (14), we get:

$$\begin{aligned} (p - p_b)\Delta x \Delta y &\ge \sigma'_{z0}\Delta x \Delta y + 2\Delta y \left\{\frac{1}{2}(\gamma_s - \gamma_w)z^2 \tan\phi - cz\right\} u(\sigma'_{x0}) \\ &+ 2\Delta x \left\{\frac{1}{2}(\gamma_s - \gamma_w)z^2 \tan\phi - cz\right\} u(\sigma'_{y0}) \end{aligned} \tag{16}$$

for sandy soil, cohesion $c = 0$, the above liquefaction criteria becomes

$$\begin{aligned} (p - p_b) &\ge \sigma'_{z0} + \frac{z^2}{\Delta y}\{(\gamma_s - \gamma_w)\tan\phi\}u(\sigma'_{x0}) \\ &+ \frac{z^2}{\Delta x}\{(\gamma_s - \gamma_w)\tan\phi\}u(\sigma'_{y0}) \end{aligned} \tag{17}$$

If the effect of $\sigma'_{x0}$ and $\sigma'_{y0}$ on the liquefaction potential is not considered, the liquefaction criteria Eq. (17) can be degenerated to the 1D liquefaction criteria based on the dynamic pore pressure proposed by Zen and Yamazaki [26] (criteria *B*). The liquefaction criteria proposed by Jeng [9]) (criteria *D*) just make an average of the initial effective stresses to consider the effect of $\sigma'_{x0}$ and $\sigma'_{y0}$ on the liquefaction resistance. There is no clear physical basis to demonstrate how the $\sigma'_{x0}$ and $\sigma'_{y0}$ affect the liquefaction potential of soil. In criteria *E* proposed in this study, the effect of $\sigma'_{x0}$ and $\sigma'_{y0}$ on the liquefaction potential is taken into consideration by estimating the lateral friction induced by $\sigma'_{x0}$ and $\sigma'_{y0}$ through the Mohr–Coulomb law. From the view of physics, the criteria *E* is much more reasonable than the criteria *D*. From Eq. (17), it can be known that the resistance to liquefaction induced by $\sigma'_{x0}$ and $\sigma'_{y0}$ is positively related to the depth $z$. Criteria *E* proposed here cannot be degenerated to the criteria *D* proposed by Jeng [9].

Unfortunately, the most difficult problem suffered in application of criteria *E* is that how to determine the size of $\Delta x$ and $\Delta y$. From Eq.

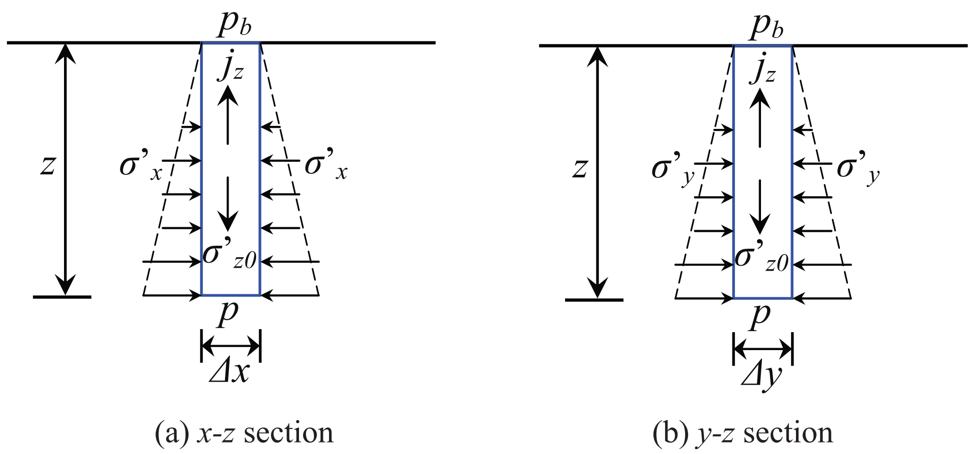


**Fig. 2.** The schematic diagram of force on a macro 3D soil volume.

(17), we know that the large $\Delta x$ and $\Delta y$ would make the effect of $\sigma'_{x0}$ and $\sigma'_{y0}$ decrease, and small $\Delta x$ and $\Delta y$ would make the effect of $\sigma'_{x0}$ and $\sigma'_{y0}$ significantly increase. Therefore, to authors' knowledge, the liquefaction criteria *E* (Eq. (17)) actually is not applicable to directly judge the liquefaction of soil due to the existence of $\Delta x$ and $\Delta y$. However, the liquefaction criteria *E* proposed in this study at least indicates that criteria *D* [9] adopting the mean initial effective stresses is not reasonable from the view of physics.

Comparing the criteria *B*, *D* and *E*, it is found that the maximum liquefaction depth in seabed under wave loading predicted by criteria *B*, *D* and *E*, respectively has following sequence: $d_E \le d_B \le d_D$. $d_B \le d_D$ is because the mean value of initial effective stresses generally is less than the initial vertical effective stress $\sigma'_{z0}$ at a certain depth. $d_E \le d_B$ attributes to that the lateral friction induced by $\sigma'_{x0}$ and $\sigma'_{y0}$ could effectively prevent the liquefaction advancing downward. From the view of physics, the liquefaction depth determined by criteria *E* proposed in this study is most reliable. However, this liquefaction depth cannot be quantitatively determined. The liquefaction depth predicted by the criteria *D* [9] would significantly overestimated. Therefore, the 1D liquefaction criteria *B* proposed by Zen and Yamazaki [26] may be the best choice in engineering. On the one side, criteria *B* is easy to use. On the other hand, the predicted liquefaction depth is relatively conservative for engineering design.

For the seabed with marine structures, due to that the initial effective stresses in seabed foundation will be significantly affected by the weight of marine structures, the initial effective stress $\sigma'_{x0}$, $\sigma'_{y0}$ and $\sigma'_{z0}$ cannot be described by Eq. (15), Eq. (14) only can be simplified as:

$$(p - p_b) \ge \sigma'_{z0} + \frac{1}{\Delta x}\int_z^0 2(c + \sigma'_{x0}\tan\phi)u(\sigma'_{x0})dz + \frac{1}{\Delta y}\int_z^0 2(c + \sigma'_{y0}\tan\phi)u(\sigma'_{y0})dz \tag{18}$$

It is the same like that situation without marine structure built on seabed, the maximum liquefaction depth predicted by criteria *B*, *D* and Eq. (18) is: $d_E \le d_B \le d_D$. The reason is the same with that without marine structure built on seabed. Therefore, it is also recommended that the 1D criteria proposed by Zen and Yamazaki [26] could be used in engineering design.

The liquefaction in seabed floor can be induced by earthquake or ocean wave loading. If the above proposed 3D liquefaction criteria is adopted to access the wave induced liquefaction in a seabed floor, generally, the seabed floor and ocean wave in the offshore environments, where the water depth normally is not deeper than 50 m, are defaulted as the investigation objects. In the deep ocean, the wave effect on the seabed floor is minor. There is no need to study the seabed response under wave loading. In the real offshore environments, the seabed generally consists of sandy soil or silty soil. The new proposed 3D liquefaction criteria are applicable both for the sandy soil and silty soil. The different between the sandy soil and silty soil in the proposed liquefaction criteria is that: the cohesion is zero for sandy soil, while, it is not zero for silty soil.

## 3. Comparisons: the wave–current induced seabed liquefaction

Due to the fact that the ocean wave and current generally coexist in the offshore environment, in this section, the liquefaction of seabed under wave and uniform current loading is taken as an example to demonstrate the differences of shape, area and depth of liquefaction zone predicted by the liquefaction criteria *A*, *B*, *C*, *D* and *E*.

Hsu et al. [6] proposed a third-order analytical solution for the wave and uniform current interaction by adopting the perturbation theory. The solution of free surface $\eta$ are expressed as:

$$\begin{aligned}\eta &= \frac{1}{2}H\cos(\lambda x - \omega t) \\ &+ \frac{1}{16}\lambda H^2\frac{(3 + 2\sinh^2(\lambda d)\cosh(\lambda d)}{\sinh^3(\lambda d)}\cos 2(\lambda x - \omega t) \\ &+ \frac{1}{16}\lambda^2\left(\frac{1}{2}H\right)^3\frac{(3 + 14\sinh^2(\lambda d) + 2\sinh^4(\lambda d))}{\sinh^4(\lambda d)}\cos(\lambda x - \omega t) \\ &+ \frac{1}{64}\lambda^2\left(\frac{1}{2}H\right)^3\frac{27 + 72\sinh^2(\lambda d) + 72\sinh^4(\lambda d) + 24\sinh^6(\lambda d)}{\sinh^6(\lambda d)}\cos 3(\lambda x - \omega t)\end{aligned} \tag{19}$$

where the *H* is the wave height of first-order wave, $\lambda$ is the wave number, *d* is the water depth, $U_0$ is the current velocity, *g* is the gravity.

The nonlinear dispersion relation is:

$$\omega = \omega_1 + \frac{1}{64}\lambda^2 H^2(\omega_1 - U_0\lambda)\frac{9 + 8\sinh^2(\lambda d) + 8\sinh^4(\lambda d)}{\sinh^4(\lambda d)} \tag{20}$$

$$\omega_1 = U_0\lambda + \sqrt{gk\tanh(\lambda d)} \tag{21}$$

The dynamic pressure acting on the seabed is:

$$\begin{aligned}P_b(x,t)= &\frac{\rho_f gH}{2\cosh\lambda d}\left[1-\frac{\omega_2\lambda^2H^2}{2(U_0\lambda-\omega_0)}\right]\cos(\lambda x-\omega t)\\ &+\frac{3\rho_f H^2}{8}\left\{\frac{\omega_0(\omega_0-U_0\lambda)}{2\sinh^4(\lambda d)}-\frac{g\lambda}{3\sinh 2\lambda d}\right\}\cos 2(\lambda x-\omega t)\\ &+\frac{3\rho_f\lambda H^3\omega_0(\omega_0-U_0\lambda)}{512}\frac{(9-4\sinh^2(\lambda d))}{\sinh^7\lambda d}\cos 3(\lambda x-\omega t)\end{aligned} \tag{22}$$

where $\rho_f$ is the density of sea water. This wave–uniform current induced pressure acting on seabed $p_b$ is the boundary condition for the dynamic response of seabed soil.

The dynamic response of seabed under wave and uniform current loading has been investigated by Ye and Jeng [24] adopting the integrated numerical model PORO-WSSI II, which is developed by Ye [22] and Jeng et al. [10] for the problem of wave–seabed–marine structures interaction. In the integrated model PORO-WSSI II, the FEM soil model DIANA SWANDYNE II developed by Chan [3], which originally was for the dynamic response of soil under seismic loading, rather than the wave loading, and the wave model COBRAS developed by Liu's groud in Conell University [8,12,13] are coupled together. This integrated model has been verified and validated extensively using experimental tests data in Ref. [22]. More detailed information can be referred to Ye [22], Ye and Jeng [24] and Ye and Jeng [23]. Here, the integrated model PORO-WSSI II also adopted to determine the stress status of seabed, and further predict the liquefaction zone in seabed by using different criteria.

The governing equation used in integrated model PORO-WSSI II for the porous seabed (plain strain) is the Biot's dynamic equation known as "$u-p$" approximation proposed by Zienkiewicz et al. [28]:

$$\frac{\partial\sigma'_x}{\partial x}+\frac{\partial\tau_{xz}}{\partial z}=-\frac{\partial p_s}{\partial x}+\rho\frac{\partial^2u_s}{\partial t^2}, \tag{23}$$

$$\frac{\partial\tau_{xz}}{\partial x}+\frac{\partial\sigma'_z}{\partial z}+\rho g=-\frac{\partial p_s}{\partial z}+\rho\frac{\partial^2w_s}{\partial t^2}, \tag{24}$$

$$k\nabla^2p_s-\gamma_w n\beta\frac{\partial p_s}{\partial t}+k\rho_f\frac{\partial^2\epsilon}{\partial t^2}=\gamma_w\frac{\partial\epsilon}{\partial t}, \tag{25}$$

where $(u_s, w_s)$ is the the soil displacements in the horizontal and vertical directions, respectively; $n$ is soil porosity; $\sigma'_x$ and $\sigma'_z$ are effective normal stresses in the horizontal and vertical directions, respectively; $\tau_{xz}$ is shear stress; $p_s$ is pore water pressure; $\rho=\rho_f n+\rho_s(1-n)$ is average density of porous seabed; $\rho_f$ is fluid density; $\rho_s$ is solid density; $k$ is Darcy's permeability; $g$ is gravitational acceleration and $\epsilon$ is the volumetric strain. In Eq. (24), the compressibility of pore fluid ($\beta$) and the volume strain ($\epsilon$) are defined as

$$\beta=\left(\frac{1}{K_f}+\frac{1-S_r}{p_{w0}}\right),\quad\text{and}\quad\epsilon=\frac{\partial u_s}{\partial x}+\frac{\partial w_s}{\partial z}, \tag{26}$$

where $S_r$ is the degree of saturation of seabed, $p_{w0}$ is the absolute static pressure and $K_f$ is the bulk modulus of pore water.

The computational domain is a seabed without marine structure truncated from the infinite seabed. The length of computational domain is equal to the wave length. The thickness of seabed is 20 m. The periodical boundary condition is applied to the two lateral sides of seabed; and the bottom of seabed is rigid and impermeable. The water pressure determined by the three-order theory mentioned above is applied to the seabed surface. The properties of seabed are: Young's modulus $E=3.0\times10^7$ Pa, Poisson's ration $\nu=0.33333$, saturation $S_r=98\%$, permeability $k=1.0\times10^{-4}$ m/s, the internal friction angle $\phi$=35°, and the cohesion $c=0$ for sandy soil. The wave height $H=3.0$ m, wave period $T=10.0$ s, water depth $d=10$ m, the velocity of current $U_0$ is 1.0 m/s. Accordingly, the wave length $L$ is determined as 108.13 m. It is noted that the compression is taken as negative in PORO-WSSI II.

### 3.1. Consolidation

In real offshore environment, the seabed generally has sufficiently experienced the consolidation process in the long-term geological history. There is no excess pore pressure in seabed under the hydrostatic pressure loading only. This final consolidation status should be taken as the initial condition for the thereafter dynamic analysis. Furthermore, the initial geostress, namely the effective stresses $\sigma'_{x0}$, $\sigma'_{y0}$ and $\sigma'_{z0}$ in seabed soil can be determined in this consolidation status.

Fig. 3 shows the distribution of initial geological effective stress $\sigma'_{x0}$, $\sigma'_{y0}$ and $\sigma'_{z0}$ in seabed under hydrostatic pressure (water depth $d=10$ m) after the consolidation process finish completely. Due to the fact that there is no marine structure built on seabed, the stress field in the seabed is not affected by external loading. The distribution of initial geological effective stresses in seabed is layered. The horizontal effective stress $\sigma'_{x0}$, $\sigma'_{y0}$ generally are half of the vertical effective stress $\sigma'_{z0}$. The lateral compression coefficient is about $K_0=0.5$ for homogenous and isotropic seabed floor. The pore pressure in seabed is also layered, and there is no excess pore pressure.

### 3.2. Dynamic response

Taking the initial geological consolidation status as the initial condition, and applying the wave–uniform current induced pressure on seabed to the surface of computational domain, the dynamic response of seabed is calculated by adopting the integrated model PORO WSSI II. Here, the dynamic seabed response under wave and current loading at time $t=30$ s is taken as a representative to illustrate the problem.

Fig. 4 is the wave profile for the wave ($H=3.0$ m, $T=10.0$ s, and $d=10.0$ m) and following current ($U_0=1.0$ m/s) at time $t=30$ s. It is clearly observed that the nonlinear characteristics are obvious for the wave and current interaction. There are fluctuations of the wave profile in the wave troughs. These fluctuations also can be seen in Hsu et al. [7] and Jian et al. [11] when the $\lambda H\geq0.2$. The range of seabed chosen as computational domain is 0–108.13 m. It can be found that the part of seabed near to the two lateral sides is applied by the wave crest; meanwhile, the middle part of seabed is applied by the wave trough.

Fig. 5 is the dynamic response of seabed under the wave and uniform current loading at time $t=30$ s. As illustrated in Fig. 5, the dynamic pore pressure $p_{sd}$ is positive, and the dynamic effective stress $\sigma'_{xd}$, $\sigma'_{yd}$ and $\sigma'_{zd}$ are compressive in the part under wave crest; while, the dynamic pore pressure $p_{sd}$ is negative, and the dynamic effective stress $\sigma'_{xd}$, $\sigma'_{yd}$ and $\sigma'_{zd}$ are tensile in the part under wave trough. Due to the fact that the wave crest downward compresses the seabed, and the wave trough relatively upward pulls the seabed, the seabed under wave trough is more likely to liquefy.

A interesting phenomenon can be observed in Fig. 5 is that it seems that there is a border line at $z=18$ m in seabed. The dynamic response of seabed in the zones $z$>18 m and $z$<18 m is significantly different. The magnitude of dynamic pore pressure in the zone $z$> 18 m is much greater than that in the zone $z$< 18 m. There is obvious phase lag for the dynamic response in the zone $z$< 18 m relative to the dynamic response in the zone $z$> 18 m. Due to the fact that the wave and current induced liquefaction in seabed would only occur at the seabed surface region, the dynamic response in the zone $z$> 18 m really need to pay our attention. Fig. 6 more clearly shows the dynamic response in the zone $z$> 18 m at time $t=30$ s.

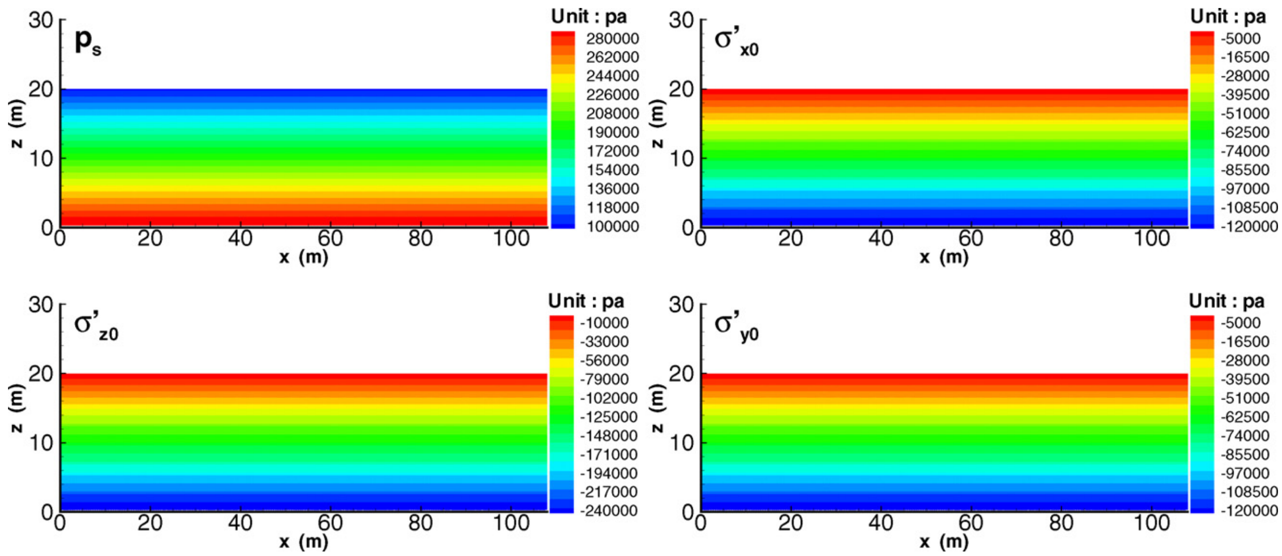


**Fig. 3.** The distribution of the effective stresses $\sigma'_{x0}$, $\sigma'_{y0}$, $\sigma'_{z0}$ and the pore pressure in seabed after consolidation.

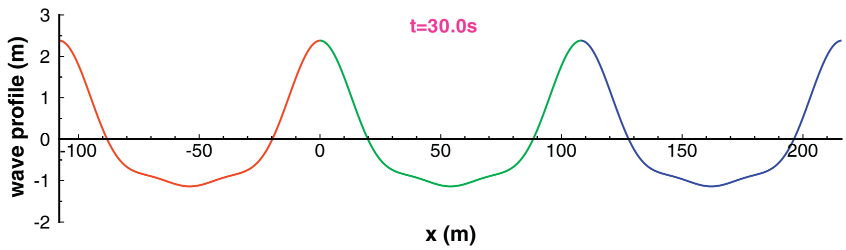


**Fig. 4.** The wave profile of the wave–current propagating on seabed at time $t = 30$ s. $H = 3.0$ m, $T = 10.0$ s, $d = 10.0$ m and $U_0 = 1.0$ m/s.

In order to completely show the dynamic stress field in seabed under wave and current loading, the distribution of shear stress $\tau_{xzd}$ in seabed is shown in Fig. 7. From Fig. 7, it is found that the there is basically no shear stress in the zone $z > 18$ m. The magnitude of shear stress $\tau_{xzd}$ in seabed is symmetrical along $x = 54.065$ m due to that the wave and current is symmetrical, the seabed and boundary conditions applied are also symmetrical.

### 3.3. Liquefaction in seabed

As mentioned above, the seabed under wave crest is compressed by the wave–current induced pressure; and the sea water will flow into the seabed driven by the pressure gradient generated due to the phase lag between the pressure acting on seabed and the induced pore pressure in seabed. The induced downward seepage

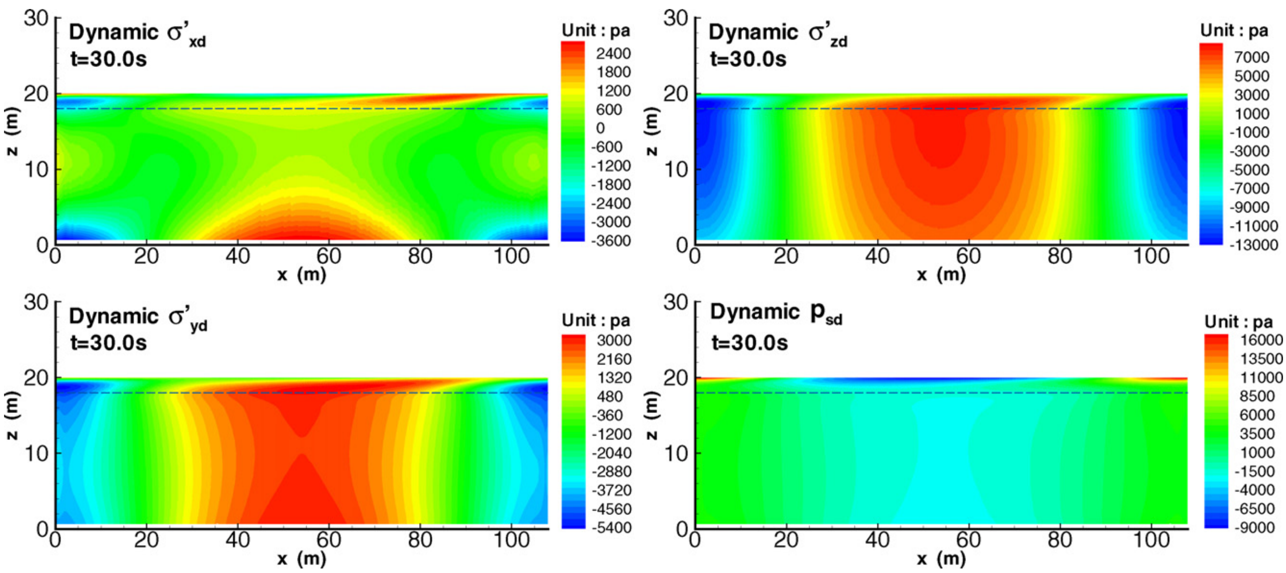


**Fig. 5.** The distribution of the wave–current induced effective stresses $\sigma'_x$, $\sigma'_y$, $\sigma'_z$ and the pore pressure in seabed at time $t = 30$ s.

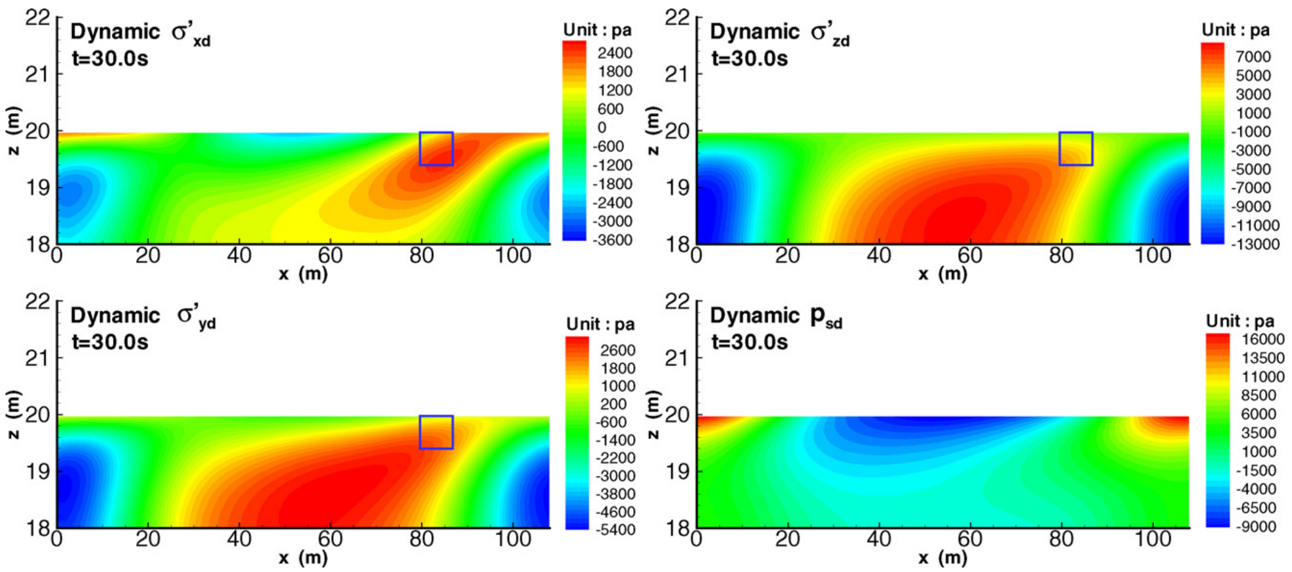


**Fig. 6.** The distribution of the wave–current induced effective stresses $\sigma_x'$, $\sigma_y'$, $\sigma_z'$ and the pore pressure in the upper seabed at time $t = 30$ s.

force make the effective stresses increase. Therefore, it is impossible for the seabed under wave crest to liquefy. However, the situation is completely opposite for the seabed under wave trough. The phase lag between the pressure acting on seabed and the pore pressure in seabed makes the seepage force is upward, which further makes the effective stresses decrease. When the driven force could overcome the initial vertical effective stress $\sigma_{z0}'$ and the lateral friction force provided by $\sigma_x'$, $\sigma_y'$, the seabed will liquefy. The phase lag induced seepage force in seabed play important role in the analysis of liquefaction of seabed. The seepage force is defined as

$$j_x = \frac{\partial p_s}{\partial x} \quad \text{and} \quad j_z = \frac{\partial p_s}{\partial z} \tag{27}$$

and

$$j = \sqrt{j_x^2 + j_z^2} \tag{28}$$

Fig. 8 shows the distribution of seepage force in seabed under wave and uniform current loading at time $t = 30$ s. It can be clearly observed that the seepage force is downward in the part near to the two lateral sides under wave crest; meanwhile, the seepage force is upward in the middle part of seabed under wave trough. The existence of tail in the seepage force distribution in seabed also indicates that the there is obvious phase lag between the pressure acting on seabed and the pore pressure in seabed; and the magnitude of phase lag is positively related to the depth of position.

Fig. 9 illustrates the liquefaction zone in seabed under the wave and uniform current loading at time $t = 30$ s by respectively adopting the liquefaction criteria *A*, *B*, *C*, *D* and *E* (here, the criteria *F* is not adopted due to the difficulty of determining the $\Delta x$ and $\Delta y$). From Fig. 9, it can be seen that the positions, shapes and sizes of the liquefaction zone predicted by different liquefaction criteria are significantly different.

The liquefaction depth (denoted as *d*) and area (denoted as *a*) in seabed predicted by criteria *A*, *C* and *E* has relationship: $d_A > d_C > d_E$ and $a_A > a_C > a_E$. This attributes to that the criteria *A* does not consider the liquefaction prevention provided by the $\sigma_x'$, $\sigma_y'$; and the criteria *C* assumes the internal friction of sandy soil is only $\phi = 26.6°$. Here, the $\phi = 35°$ is used for sandy soil in criteria *E*. It is indicated that the criteria *A* and *C* would overestimate the liquefaction depth and area in engineering.

It is clearly observed in Fig. 9 that the liquefaction depth and area is greatly overestimated by criteria *D* compared with that predicted by the criteria *B*. As the analysis in Section 2.2, criteria *D* just takes the average of initial geological effective stresses as the liquefaction resistance; the physical basis of how the initial horizontal effective stresses $\sigma_{x0}'$, $\sigma_{y0}'$ affect the liquefaction resistance is not clear. Criteria *F* proposed in this study cannot be degenerated to the criteria *D*. Due to the fact that the average of initial effective stresses is generally less than the initial vertical effective stress, the greatly overestimated liquefaction depth and area predicted by criteria *D* is undoubtedly expected. In engineering, the liquefaction criteria *D* is not recommended to use.

Fig. 10 is the historic curve of liquefaction depth on line $x = 75.0$ m using different liquefaction criteria. Fig. 10 also shows that the liquefaction depth predicted by criteria *D* is much greater than that predicted by other criteria; and the duration of liquefaction in one wave period on line $x = 75.0$ m is longest. It is also

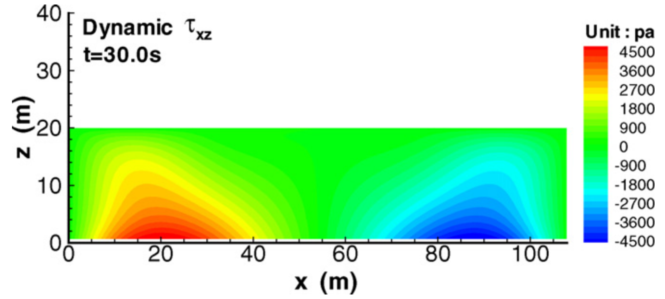


**Fig. 7.** The distribution of the wave–current induced shear stress $\tau_{xz}$ in seabed at time $t = 30$ s.

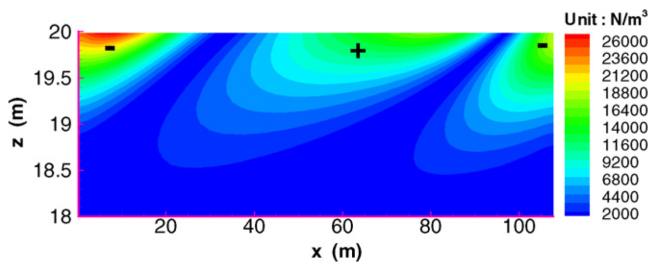


**Fig. 8.** The distribution pf seepage force in seabed at time $t = 30$ s. The '+' means upward seepage force; '–' means downward seepage force.

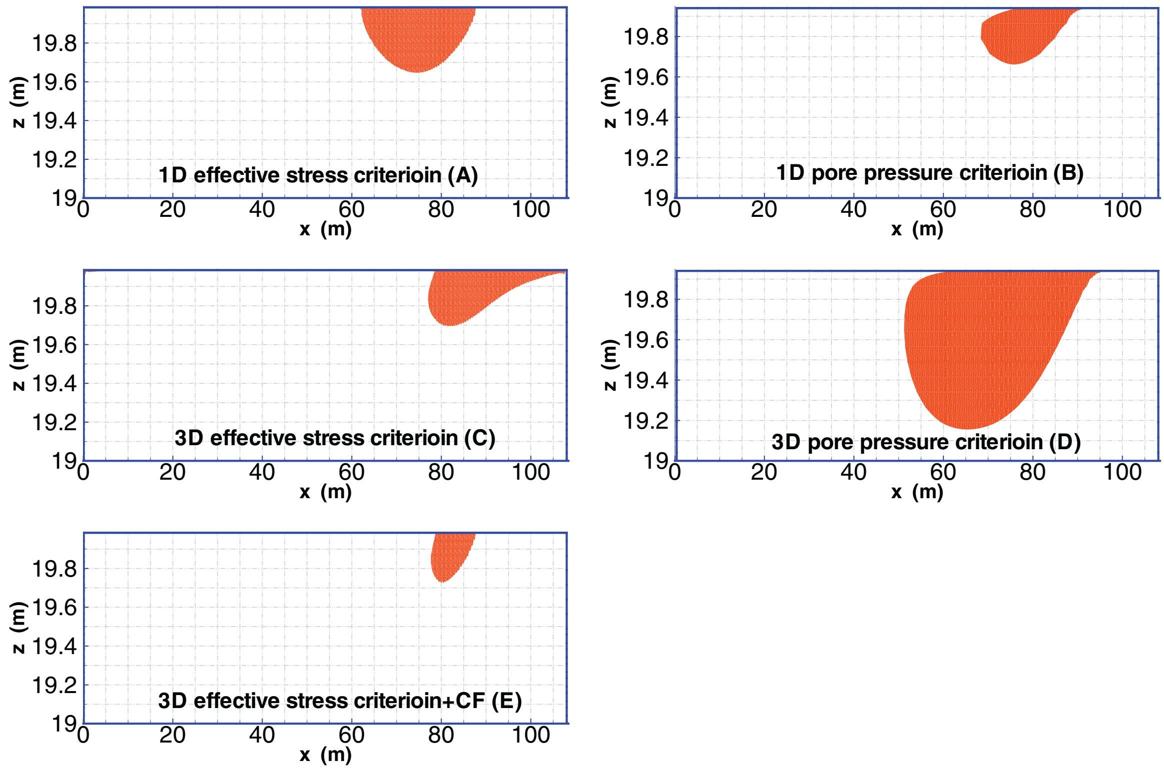


**Fig. 9.** The liquefaction zones in seabed predicted by different liquefaction criteria at time $t = 30$ s. $H = 3$m, $T = 10$ s, $d = 10$ m, $U_0 = 1$ m/s, $c = 0$, $\phi = 35^{\circ}$.

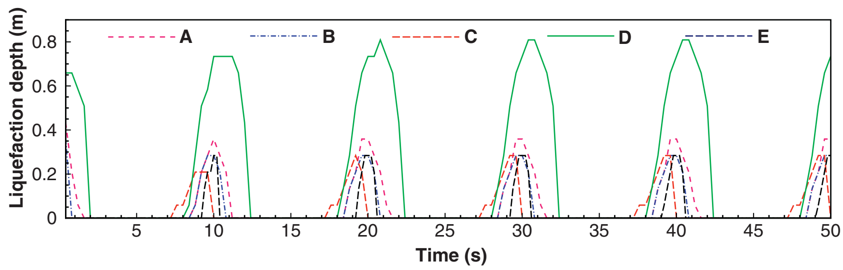


**Fig. 10.** The historic curve of liquefaction depth in seabed on line $x = 75.0$ m using different liquefaction criteria.

observed that the maximum liquefaction depth on line $x = 75.0$ m is basically the same predicted by the criteria *B*, *C* and *E*; however, the start time and duration of liquefaction on line $x = 75.0$ m is different. The duration of liquefaction predicted by criteria *E* is the shortest one.

## 4. Conclusions

In this study, according to the Mohr–Coulomb principle, the liquefaction criteria considering the cohesion and internal friction angle of soil are proposed based on the effective stress state, and the dynamic loading induced pore pressure in seabed. Through the comparison investigation, following understanding are obtained:

(1) The cohesion and internal friction angle of soil indeed have significant effect on the prediction of liquefaction zone in seabed under dynamic loading. It is necessary to consider the cohesion and internal friction angle when evaluation of the liquefaction potential of soil foundation.

(2) The liquefaction criteria *E* proposed in this study based on the effective stress state can be degenerated to the 1D liquefaction criteria *A* proposed by Okusa [16] if the cohesion and friction angle are both neglected. The liquefaction criteria *E* also can be degenerated to the liquefaction criteria *C* proposed by Tsai [20] if the cohesion is ignored, and the internal friction angle is assumed as $\phi = 26.6^{\circ}$. The area and maximum depth of liquefaction zone predicted by liquefaction criteria *A*, *C* and *E* have following relationship: $a_A \geq a_C \geq a_E$, and $d_A \geq d_C \geq d_E$. The liquefaction zone predicted by criteria *E* would be the most accurate one among the three criteria based on the effective stress state. In engineering, the 1D liquefaction criteria *A* proposed by Okusa [16] also can be used due to that some appropriate safe margin could be left for the structures stability.

(3) The liquefaction criteria *F* proposed in this study based on the dynamic pore pressure can be degenerated to the 1D liquefaction criteria *B* proposed by Zen and Yamazaki [26] if the cohesion and internal friction angle of soil are not considered. However, The liquefaction criteria *F* cannot be degenerated to liquefaction criteria *D* proposed by Jeng [9]. Therefore, the averaging of the initial effective stresses in the liquefaction criteria *D* have not physical basis. Additionally, the area and maximum depth of liquefaction zone in seabed is overestimated greatly. It is not recommended to use the liquefaction criteria *D* in engineering.

(4) Due to the fact that the distribution of initial horizontal effective stresses $\sigma'_{x0}$ and $\sigma'_{y0}$ in seabed under marine structures

is generally unknown, the liquefaction criteria $F$ is also not applicable. The 1D criteria proposed by Zen and Yamazaki [26] is recommended to used in engineering, if the dynamic pore pressure in seabed foundation need to be used.

## References


[1] Boulanger RW, Idriss IM. Liquefaction susceptibility criteria for silts and clays. Journal of Geotechnical and Geoenvironmental Engineering 2006;132(11):1413–26.
[2] Bray DJ, Sancio RB. Assessment of the liquefaction susceptibility of fine-grained soils. Journal of Geotechnical and Geoenvironmental Engineering 2006;132(9):1165–77.
[3] Chan AHC. A unified finite element solution to static and dynamic problems of geomechanics. PhD thesis. Swansea Wales: University of Wales; 1988.
[4] Chung SG, Kim SK, Kang YJ, Im JC, Prasad KN. Failure of a breakwater founded on a thick normally consolidated clay layer. Géotechnique 2006;56(3):393–409.
[5] Franco L. Vertical breakwaters: the Italian experience. Coastal Engineering 1994;22(1-2):31–55 [special issue Vertical Breakwaters].
[6] Hsu HC, Chen YY, Hsu JRC, Tseng WJ. Nonlinear water waves on uniform current in Lagrangian coordinates. Journal of Nonlinear Mathematical Physics 2009;16(1):47–61.
[7] Hsu JRC, Tsuchiya Y, Silvester R. Third-order approximation to short-crested waves. Journal of Fluid Mechanics 1979;90(Part 1):179–96.
[8] Hsu TJ, Sakakiyama T, Liu PLF. A numerical model for wave motions and turbulence flows in front of a composite breakwater. Coastal Engineering 2002;46:C25–50.
[9] Jeng D-S. Wave-induced seabed response in front of a breakwater. PhD thesis. Perth, Australia: University of Western Australia; 1997.
[10] Jeng D-S, Ye JH, Liu PF. An integrated model for the wave–seabed–structures interaction – model, verifications and application. Coastal Engineering, submitted for publication.
[11] Jian YJ, Zhu QY, Zhang J, Wang YF. Third order approximation to capillary gravity short crested waves with uniform currents. Applied Mathematical Modelling 2009;33(4):2035–53.
[12] Lin P, Liu PLF. A numerical study of breaking waves in the surf zone. Journal of Fluid Mechanics 1998;359:239L 264.
[13] Lin ZP, Liu PL-F. Internal wave-maker for Navier–Stokes equations models. Journal of Waterway, Port, Coastal, and Ocean Engineering 1999;99(4): 207–15.
[14] Lundgren H, Lindhardt JHC, Romold CJ. Stability of breakwaters on porous foundation. In: Proceeding of 12th international conference on soil mechanics and foundation engineering, vol. 1. 1989. p. 451–4.
[15] Muhunthan B, Worthen DL. Critical state framework for liquefaction of fine grained soils. Engineering Geology 2011;117(1–2):2–11.
[16] Okusa S. Wave-induced stress in unsaturated submarine sediments. Geotechnique 1985;35(4):517–32.
[17] Seed HB, Idriss IM. Ground motions and soil liquefaction during earthquakes. Technical report. Berkerlay, California: Earthquake Engineering Research Institute; 1979.
[18] Silvester R, Hsu JRC. Sines revisited. Journal of Waterway, Port, Coastal, Ocean Engineering, ASCE 1989;115(3):327–44.
[19] Sumer BM, Ansal A, Cetin KO, Damgaard J, Gunbak AR, Hansen NEO, et al. Earthquake-induced liquefaction around marine structures. Journal of Waterway, Port, Coastal and Ocean Engineering 2007;133(1):55–82.
[20] Tsai CP. Wave-induced liquefaction potential in a porous seabed in front of a breakwater. Ocean Engineering 1995;22(1):1–18.
[21] Wang W. Some findings in soil liquefaction. Technical report. Beijing: Water Conservancy and Hydroelectirc Power Scientific Research Institute; 1979.
[22] Ye JH. Numerical analysis of wave–seabed–breakwater interactions. PhD thesis. Dundee, UK: Universtity of Dundee; 2012.
[23] Ye JH, Jeng D-S. Effects of bottom shear stresses on the wave-induced dynamic response in a porous seabed: Poro-wssi (shear) model. Acta Mechanica Sinica 2011;27(6):898–910.
[24] Ye JH, Jeng D-S. Response of porous seabed to nature loadings-waves and currents. Journal of Engineeering Mechanics, ASCE, http://dx.doi.org/10.1061/(ASCE)EM.1943-7889.0000356 in press.
[25] Zen K, Umehara Y, Finn WDL. A case study of the wave-induced liquefaction of sand layers under damaged breakwater. In: Proceeding 3rd Canadian conference on marine geotechnical engineering. 1985. p. 505–20.
[26] Zen K, Yamazaki H. Oscillatory pore pressure and liquefaction in seabed induced by ocean waves. Soils and Foundations 1990;30(4):147–61.
[27] Zhang FG, Ge ZJ. A study on some causes of rubble mound breakwater failure. China Ocean Engineering 1996;10(4):473–81.
[28] Zienkiewicz OC, Chang CT, Bettess P. Drained, undrained, consolidating and dynamic behaviour assumptions in soils. Geotechnique 1980;30(4):385–95.